Quantitative Biology 2022, 10(4): 341–350
https://doi.org/10.15302/J-QB-022-0287

RESEARCH ARTICLE

Computational study of some potential inhibitors of COVID-19: A DFT analysis

Prabhat Ranjan[1,*], Kumar Gaurav[1], Tanmoy Chakraborty[2,*]

[1] Department of Mechatronics Engineering, Manipal University Jaipur, Dehmi Kalan 303007, India
[2] Department of Chemistry and Biochemistry, School of Basic Sciences and Research, Sharda University, Greater Noida 201310, India
* Correspondence: prabhat.ranjan@jaipur.manipal.edu; tanmoy.chakraborty@sharda.ac.in

Received August 18, 2021; Revised September 13, 2021; Accepted September 16, 2021

***Background*: There is an urgent demand of drug or therapy to control the COVID-19. Until July 22, 2021 the worldwide total number of cases reported is more than 192 million and the total number of deaths reported is more than 4.12 million. Several countries have given emergency permission for use of repurposed drugs for the treatment of COVID-19 patients. This report presents a computational analysis on repurposing drugs—tenofovir, bepotastine, epirubicin, epoprostenol, tirazavirin, aprepitant and valrubicin, which can be potential inhibitors of the COVID-19.**
***Method*: Density functional theory (DFT) technique is applied for computation of these repurposed drug. For geometry optimization, functional B3LYP/6-311G (d, p) is selected within DFT framework.**
***Results*: DFT based descriptors—highest occupied molecular orbital (HOMO)-lowest unoccupied molecular orbital (LUMO) gap, molecular hardness, softness, electronegativity, electrophilicity index, nucleophilicity index and dipole moment of these species are computed. IR and Raman activities are also analysed and studied. The result shows that the HOMO-LUMO gap of these species varies from 1.061 eV to 5.327 eV. Compound aprepitant with a HOMO-LUMO gap of 1.419 eV shows the maximum intensity of IR (786.176 km mol^{-1}) and Raman spectra (15036.702 a.u.).**
***Conclusion*: Some potential inhibitors of COVID-19 are studied by using DFT technique. This study shows that epirubicin is the most reactive compound whereas tenofovir is found to be the most stable. Further analysis and clinical trials of these compounds will provide more insight.**

Keywords: COVID-19; repurposing drug; density functional theory; HOMO-LUMO; epirubicin; aprepitant

Author summary: Infection due to COVID-19 is increasing rapidly and worldwide a huge population is affected. Considering the pandemic situation and urgent demand of suitable inhibitors, researchers are looking for new compounds which could be potential drug to treat COVID-19 patients. In this report, we have investigated seven prospective inhibitors using the density functional theory (DFT) method. From this analysis, we found that tenofovir is the most stable system with maximum HOMO-LUMO energy gap.

INTRODUCTION

Currently the entire world is facing problem with the dangerous disease designated as COVID-19. As per the data up to July 22, 2021 worldwide more than 192 million cases are reported and more than 4.12 million people have lost their lives due to this disease. COVID-19 not only affects individual human life but has also paralysed the health and other sectors as well as economic conditions. It has drastically changed the life style, working culture and mental peace of many people. At present, countries like United States, India, Brazil, France, Russia, United Kingdom *etc*. are affected badly by this disease [1–8]. The coronavirus is of seven types and mainly it is classified into alpha and beta coronavirus [1]. The beta coronavirus has similar symptoms as previously identified virus such as Severe Acute Respiratory Syndrome coronavirus (SARS-CoV)

and Middle East Respiratory Syndrome coronavirus (MERS-CoV) [9,10]. On the basis of its genomic immediacy, it has been stated that SARS-CoV-2 originated from bats and entered into humans from an unidentified source [9,10].

As of now, there is no dedicated and effective drug available to control this disease. In various countries, permission has been given for emergency use of antiviral drugs to treat patients of COVID-19 [1,11–18]. Repurposed antiviral drugs have been stated to have potential value in providing an instant and economical approach to control the COVID-19 [19–21]. Some of the drugs which are being used by medical practitioners for the treatment of COVID-19 are quinine, chloroquine, lopinavir and ritonavir [1,11–18]. Researchers are also exploring for new compounds which could be potential inhibitors for against COVID-19 [19,22].

Ramkumaar *et al.* [23] have investigated tenofovir by using density functional theory (DFT) technique and found the maximum value of absorption as 286.67 nm. Patil *et al*. [24] have reported molecular docking and quantum chemical study of natural bioflavonoid resveratrol and its analogy as a potential inhibitor for COVID-19. Jarange *et al*. [25] have performed experimental as well as DFT investigation of tenofovir disoproxil fumarate with p-sulfonato-calix [4] arene and p-sulfanato-thiacalix [4] arene macrocycles. They have found that tenofovir disoproxil fumarate enters acutely into the atrium of p-sulfonato-calix [4] arene enabling hydrogen bond interlinkage between adenine protons and hydroxyl and also between methylene protons of the macrocycle. Elfiky *et al*. [26] reported the efficacy of potential drugs—ribavirin, remdesivir, sofosbuvir, galidesivir and tenofovir against SARS-CoV-2. They also pointed out the importance of guanosine derivative (IDX-184), setrobuvir and YAK for antiviral therapeutic use to fight the SARS-CoV-2. Toroz *et al*. [27] have investigated the interface among the anthracyclines and two diverse lipid bilayers (unsaturated POPC and saturated DMPC) with the help of molecular dynamics simulations, considering four anthracyclines—doxorubicin, epirubicin, idarubicin and daunorubicin. Sobczak *et al*. [28] have examined the reactivity of epidoxorubicin in solid as well as in solutions with different pH values. Samide *et al*. [29] have reported that drugs like epirubicin, gemcitabine, and paclitaxel can be used for cancer treatment. Liu *et al*. have reported some drugs like—colistin, valrubicin, icatibant, bepotastine, epirubicin, epoprostenol, vapreotide, aprepitant, caspofungin and perphenazine—which could be used for treatment of SARS-CoV-2 main protease [30]. Wang *et al*. [31] have reported some potential inhibitors—carfilzomib, eravacycline, valrubicin, loplnavir, elbasvir, streptomycin, flavin adenine dinucleotide and oftasceine, for SARS-CoV-2.

In this report, computational analysis of potential inhibitors including tenofovir, bepotastine, epirubicin, epoprostenol, tirazavirin, aprepitant and valrubicin for the COVID-19 is performed by using DFT methodology. The optimized structures of these species have real vibrational frequencies. DFT based descriptors—highest occupied molecular orbital (HOMO)-lowest unoccupied molecular orbital (LUMO) gap, molecular hardness, softness, electronegativity, electronegativity and dipole moment of these species are studied. IR and Raman activity of all the compounds are also analysed.

RESULTS

Optimized structure

In this section, the optimized structure of species—tenofovir, bepotastine, epirubicin, epoprostenol, tirazavirin, aprepitant and valrubicin—are studied by using the density functional theory technique. The optimized structures of these species are presented in the Fig.1. Compound tenofovir with symmetry group C_1 and spin multiplicity triplet has optimization energy of –34469.875 eV. Bepotastine with symmetry group C_1 is optimized at high spin multiplicity state octet. It has optimization energy of –43781.062 eV. Compound epirubicin is optimized at singlet spin multiplicity with symmetry group C_1. The optimization energy for epirubicin is found as –52069.847 eV. Compound epoprostenol with symmetry point group C_1 is optimized at high spin multiplicity state *i.e.* octet. It has optimization energy of –31448.496 eV. Tirazavirin with symmetry group C_1 and singlet spin multiplicity has optimization energy of –20588.008 eV. Compound aprepitant with symmetry group C_1 is optimized at high spin multiplicity state *i.e.* octetha and has optimization energy of –54956.637 eV. Compound valrubicin with symmetry group C_1 and spin multiplicity state singlet has optimization energy of –72057.470 eV.

Density functional theory based descriptors

Computational study of some potential inhibitors for COVID-19 is performed by using DFT technique. The DFT based global descriptors: HOMO-LUMO gap, electronegativity, hardness, softness, electrophilicity index, nucleophilicity index and dipole moment are calculated and presented in Table 1. This study's computed result shows that HOMO-LUMO of these potential inhibitors are in the range of 1.061 to 5.327 eV. Tenofovir has the maximum HOMO-LUMO gap of 5.327 eV whereas epirubicin has the smallest gap, 1.061 eV. The result shows that molecular hardness and softness of these potential inhibitors vary from 0.531 to

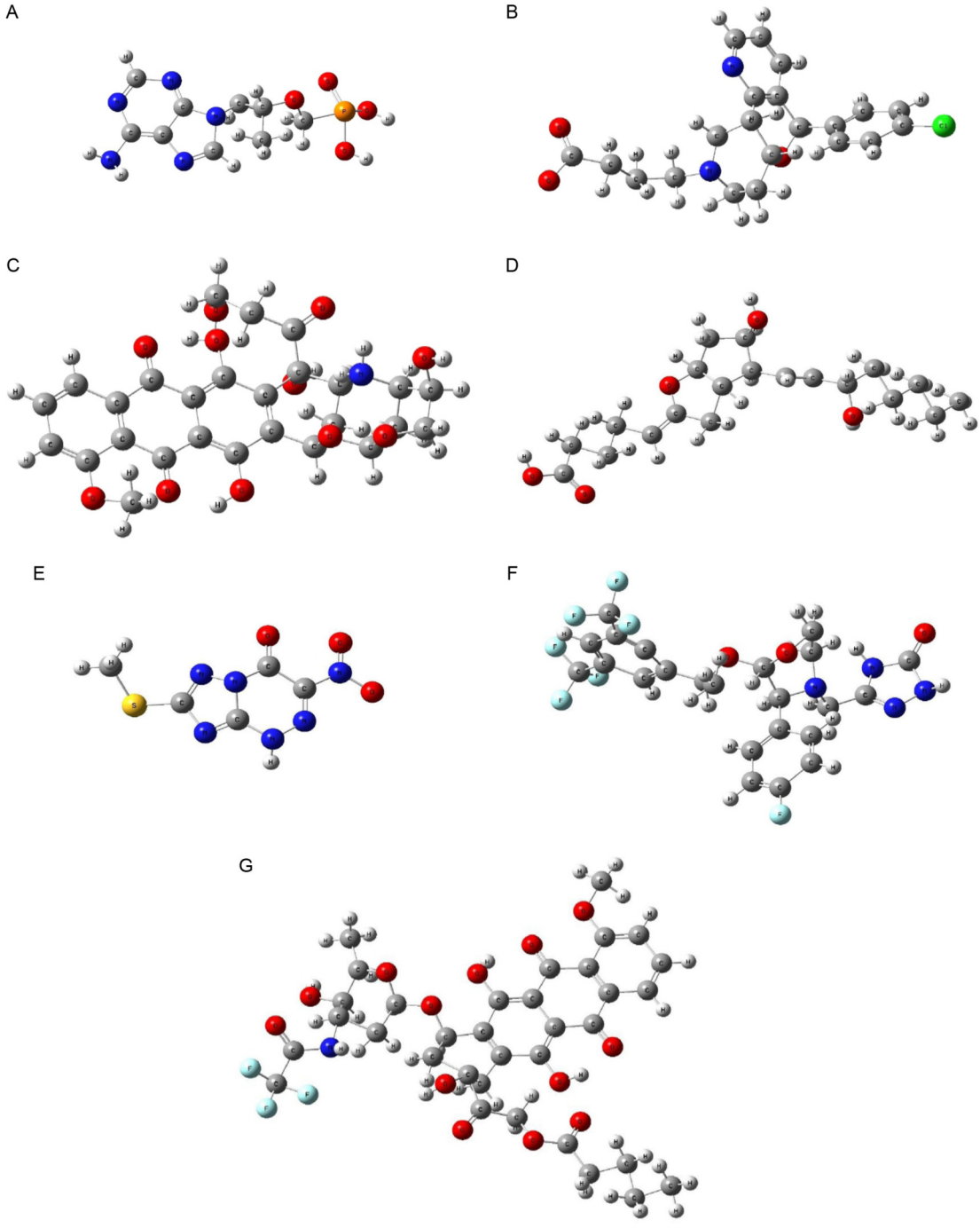

Figure 1. Optimized structure of (A–G): tenofovir, bepotastine, epirubicin, epoprostenol, tirazavirin, aprepitant and valrubicin.

2.663 eV and 0.188 to 0.942 eV respectively. Compound tenofovir with the maximum HOMO-LUMO gap shows the maximum hardness (2.663 eV) and the minimum softness value (0.188 eV), whereas epirubicin with the least HOMO-LUMO gap displays the minimum hardness (0.531 eV) and the maximum softness value (0.942 eV). Electronegativities of these species are calculated in the range of 2.427 to 5.795 eV. The maximum value of electronegativity is observed for epirubicin, 5.795 eV, whereas the minimum value is found for compound bepotastine, 2.427 eV.

The electrophilicity index and nucleophilicity index are computed in the range of 1.923 to 31.651 eV and 0.031 to 0.519 eV respectively. Epirubicin has the

Table 1 DFT based descriptors of potential inhibitors of COVID-19

Species	HOMO-LUMO gap (eV)	Hardness (eV)	Softness (eV)	Electronegativity (eV)	Electrophilicity index (eV)	Nucleophilicity index (eV)	Dipole moment (Debye)
Tenofovir	5.327	2.663	0.188	3.668	2.525	0.395	1.381
Bepotastine	2.048	1.024	0.488	2.427	2.875	0.347	1.493
Epirubicin	1.061	0.531	0.942	5.795	31.651	0.031	8.788
Epoprostenol	3.286	1.643	0.304	2.514	1.923	0.519	8.468
Tirazavirin	3.418	1.709	0.293	5.543	8.988	0.111	5.385
Aprepitant	1.419	0.710	0.705	4.972	17.423	0.057	3.135
Valrubicin	2.802	1.401	0.357	5.156	9.487	0.105	16.182

maximum electrophilicity index value, 31.651 eV, and the minimum value of nucleophilisity index, 0.031 eV. Similarly, epoprostenol has the minimum electrophilcity index value, 1.923 eV, and the maximum nucleophilicity index value, 0.519 eV. Dipole moments for these species are found in the range of 1.381 to 16.182 Debye. Valrubicin shows the maximum dipole moment of 16.182 Debye whereas tenofovir displays the least value as 1.381 Debye. The dipole moment of epirubicin (8.788 Debye) is in agreement with the data (7.5 Debye) reported by Toroz *et al*. [27].

IR and Raman spectra

In this section, IR and Raman activities of species, tenofovir, bepotastine, epirubicin, epoprostenol, tirazavirin, aprepitant and valrubicin, are studied by using B3LYP/6-311G(d, p) within density functional theory framework. IR and Raman spectra are analysed with the help of GaussSum [32]. For computing the Raman spectra, wavelength 785 nm and temperature 293 Kelvin are considered. The computed IR and Raman activities of these species are presented in Fig. 2. For compound tenofovir 93 vibrational modes are observed in the frequency range of 0 to 3773 cm^{-1}. The peak value of IR activity (570.39 km mol^{-1}) is observed at harmonic frequency 1704.39 cm^{-1}; similarly, the maximum value of Raman activity (267.28 a.u.) is found at 3090.8 cm^{-1}. The minimum value of IR intensity *i.e.* 0.4390 km mol^{-1} and Raman spectra *i.e.* 0.177 a.u. occur at harmonic frequencies 61.180 and 81.300 cm^{-1} respectively. Bepotastine has 147 vibrational modes in the frequency range of 0 –3320 cm^{-1}. The maximum values of IR activity (316.05 km mol^{-1}) and Raman spectra (293.98 a.u.) are observed at 2276.88 and 3161.86 cm^{-1} respectively. At utmost harmonic frequency, IR intensity of 17.22 km mol^{-1} and Raman spectra of 96.359 a.u. is found. The smallest intensities of IR (0.0061 km mol^{-1}) and Raman (0.222 a.u.) are observed at 2.078 cm^{-1}. There are 132 vibrational modes identified for epirubicin in the range of 0 –3737.68 cm^{-1}. High intensity of IR and Raman spectra is observed as 761.084 km mol^{-1} and 5626.4 a.u. at harmonic frequencies 2388.25 and 1461.29 cm^{-1} respectively. At the maximum frequency IR intensity of 152.167 km mol^{-1} and Raman spectra of 63.77 a.u. is observed. The lowest values of IR intensity (0.396 km mol^{-1}) and Raman spectra (0.734 a.u.) are found at 211.822 and 36.177 cm^{-1} respectively. For compound epoprostenol 162 vibrational modes are found in the range of 0–4447.04 cm^{-1}. The peak intensities of IR and Raman spectra are observed as 178.404 km mol^{-1} and 3105.08 a.u. at 1241.52 and 1639.74 cm^{-1} respectively. The least value of IR (0.004 km mol^{-1}) and Raman (0.056 a.u.) is found at 14.262 cm^{-1}. At the maximum frequency, low intensity of IR (8.848 km mol^{-1}) and Raman spectra (99.940 a.u.) are observed. For compound tirazavirin 51 vibrational modes are found in the range of 0 to 3741.48 cm^{-1}. Peak intensity of IR, 318.812 km mol^{-1}, is observed at 1742.743 cm^{-1}. Two strong Raman spectra *i.e.* 142.11 a.u. and 140.986 a.u. are found at harmonic frequencies 1318.940 and 3101.820 cm^{-1} respectively. At the highest frequency, IR intensity of 167.302 km mol^{-1} and Raman activity of 105.398 a.u. are identified. The least intensity of IR (0.139 km mol^{-1}) and Raman spectra (0.107 a.u.) are found at 154.603 and 126.052 cm^{-1} respectively. In the case of aprepitant, 111 vibrational modes are observed in the range of 0 to 3766.35 cm^{-1}. The peak values of IR, 786.176 km mol^{-1}, and Raman spectra, 15036.702 a.u., are observed at 1759.49 and 1618.05 cm^{-1} respectively. IR intensity of 184.534 km mol^{-1} and Raman activity of 1824.440 a.u. are found at the maximum harmonic frequency. At the smallest value of harmonic frequency, the minimum values of IR intensity 0.080 km mol^{-1} and Raman spectra are also identified. For compound valrubicin 93 vibrational modes are found in the range of 0 to 3790.88 cm^{-1}. The maximum values of IR intensity *i.e.* 498.501 km mol^{-1} and Raman spectra *i.e.* 554.281 a.u. are found at 1690.581 and 3041.535 cm^{-1} respectively. However, the

lowest intensity of IR (0.639 km mol^{-1}) and Raman spectra (0.441 a.u.) are identified at harmonic frequencies 15.434 and 21. 552 cm^{-1} respectively. At the maximum frequency IR intensity of 33.868 km mol^{-1} and Raman spectra of 60.342 a.u. are found.

DISCUSSION

In this work, we investigated seven potential inhibitors for COVID-19. Results obtained from geometry optimization (Fig. 1) reveal that tirazavirin and valrubicin have the maximum and minimum optimization energy respectively.

The high value of HOMO indicates high tendency to contribute an electron and also high chemical reactivity. The energy difference between frontier orbitals, HOMO and LUMO, is a significant factor in inhibiting the receptor function into ligand reactivity [1]. Species with the low HOMO-LUMO gap show high chemical reactivity towards any external perturbation whereas species with high HOMO-LUMO gap will be more stable. The data presented in Table 1 shows that epirubicin is highly reactive whereas tenofovir is more stable. Molecular hardness and softness play an important role in understanding the chemical stability and reactivity of species [33,34]. Chattaraj *et al*. [35] have emphasised that molecular hardness is significant factor in study of the geometry, stability, binding and

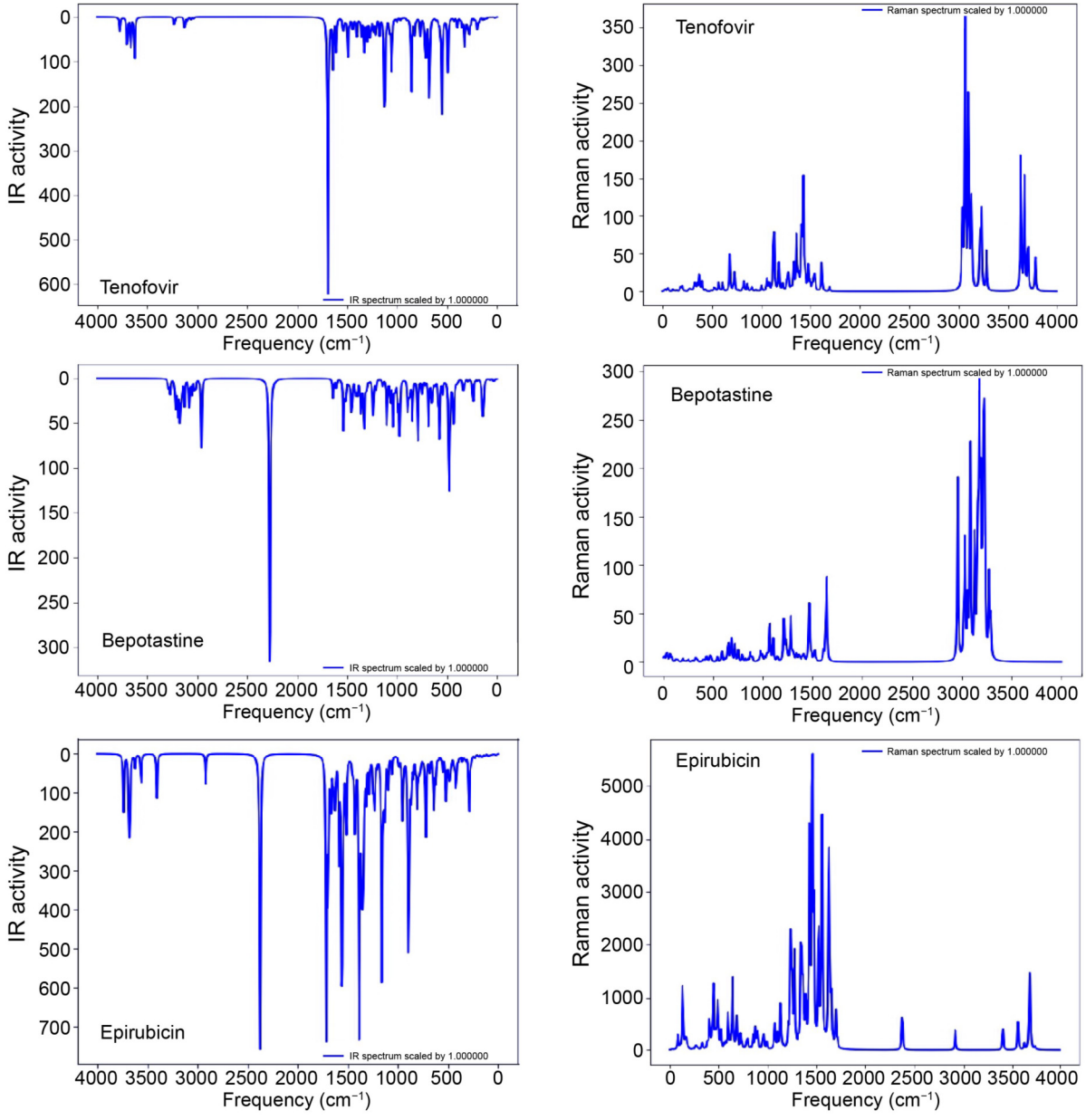

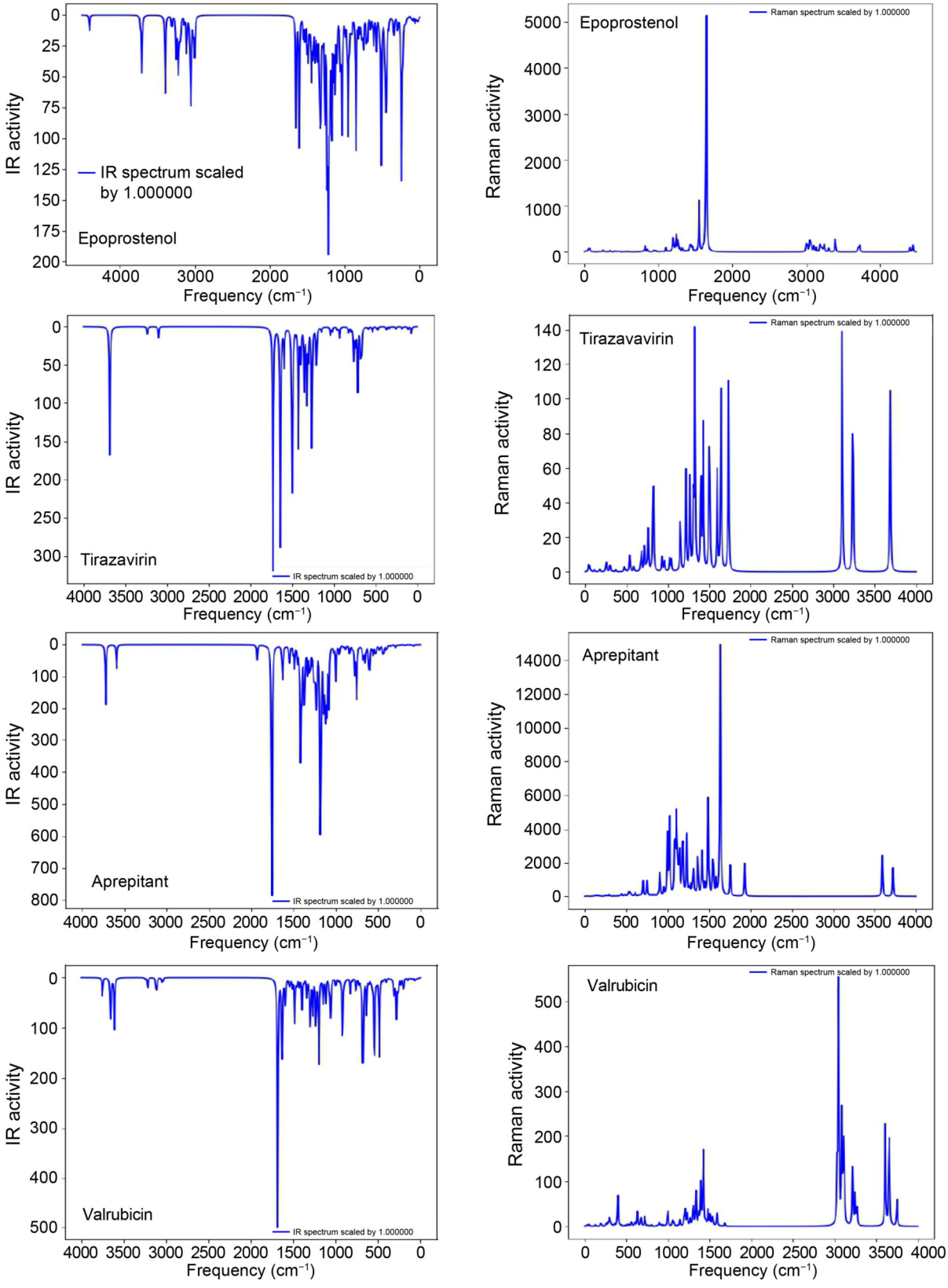

Figure 2. IR and Raman spectra of potential inhibitors of COVID-19.

dynamics of a molecular system. From Table 1, it is clear that the HOMO-LUMO gaps of these inhibitors have a direct and an inverse relation with computed hardness and softness respectively. The concept of electronegativity is important in understanding the charge transfer among donor and acceptor [36–41]. Epirubicin and bepotastine display maximum and minimum values of electronegativity respectively.

In a molecular system, electrophilicity and nucleophilicity concepts are related to electron-poor and electron-efficient respectively. An electrophile radical prefers electron-efficient locations whereas a nucleophile radical favours the electron-deficient positions to attack in the species [42]. It is already reported that the system with a high value of dipole moment will show intense aqueous solvation because of superior interface with the dipole moments of the adjoining water molecules [27]. Epirubicin and epoprostenol show the maximum and minimum value of electrophilicity index respectively. Similarly, the nucleophilicity index is found maximum and minimum for epoprostenol and epirubicin respectively. Data reveals that maximum dipole moment is found for valrubicin. It signifies that valrubicin may exhibit much greater solvation free energy in water as compared to other considered systems and hence in water phase this system may offer more stability.

Several researches have recently reported on possible COVID-19 inhibitors. For example, tenofovir has been suggested as a possible SARS-CoV-2 treatment [29]. Elfiky *et al*. [26] reported a molecular docking study of tenofovir and found good docking score value and high binding value, which reveal that it can be a promising drug for use against the COVID-19. Furthermore, study conducted on the binding affinity of numerous systems to diverse dynamic states of RdRp protein, using a molecular dynamics simulation approach, have revealed that tenofovir shows good binding energy value and it has equivalent value with respect to the four natural nucleotide triphosphates (NTPs). This signifies that it may be potential drug in the race with natural NTPs aimed at binding place of SARS-CoV-2 proteins [43]. Hasan *et al*. [44] extensively investigated a number of systems including various permitted RdRp inhibitor medicines, containing tenofovir and their structural correspondents, to search for a new probable inhibitor. They found that interfaces between those ligands and enzyme are mostly hydrophobic in nature which mixed-up residues R523, A524, R525 and r594. Authors also reveal that tenofovir shows uppermost binding affinity.

The study conducted by salpini *et al*. [45] on several permitted drugs and their metamorphosis effect on the binding affinity for the target enzyme has shown that medicines such as remdesivir display reduction in binding affinity against P323L metamorphosed RdRp; other medicines including tenofovir are found to be responsive against modified enzyme. Yun *et al*. [46] have stated that tenofovir and remdesivir display utmost docking values. It has been established that remdesivir has robust interfaces with angiotensin-converting enzyme 2 (ACE2) as compared to spike, whereas tenofovir disoproxil fumarate has shown very high response with spike protein as compared to receptor ACE2. Toor *et al*. [47] have also reported that tenofovir exhibits considerable molecular interfaces with the ACE2 for the realization of spike protein.

IR and Raman spectra (Fig. 2) reveal that maximum vibrational frequency range is obtained for compound epoprostenol whereas, minimum range of vibrational frequency is found for bepotastine. Maximum magnitude of IR spectra is observed in case of aprepitant. However, minimum IR spectra magnitude is found for compound bepotastine. Raman spectra with highest magnitude is obtained for aprepitant whereas tirazavirin display the lowest magnitude of Raman spectra.

CONCLUSION

The recent pandemic condition of COVID-19 demands search for repurposed and approved drug available commercially. Previously, it is reported that repurposing drug can be used for treatment of COVID-19 patients. In this report, authors have done a computational analysis on repurposing drugs which can be used for treatment against COVID-19—tenofovir, bepotastine, epirubicin, epoprostenol, tirazavirin aprepitant and valrubicin by using density functional theory technique. Exchange correlation B3LYP and basis set 6-311G (d, p) is used for optimization purpose. The optimized structure of all compounds has real vibrational frequencies. DFT based descriptors—HOMO-LUMO gap, molecular hardness, softness, electronegativity, electrophilicity index, nucleophiliicty index and dipole moment of these species are studied. IR and Raman activities are also studied. The HOMO-LUMO gap of these species are found in the range of 1.061 to 5.327 eV. The result reveals that epirubicin is the most reactive compound with HOMO-LUMO gap of 1.061 eV whereas tenofovir with HOMO-LUMO gap of 5.327 eV is the most stable compound. Compound aprepitant with HOMO-LUMO gap of 1.419 eV shows the maximum intensity of IR and Raman spectra.

COMPUTATIONAL DETAILS

DFT is a very popular and efficient method to study the structure and physico-chemical properties of organic compounds. Geometric optimization and physico-chemical properties play an important role in medicinal

chemistry especially for drug modelling and designing [48,49]. In this report, some potential inhibitors of COVID-19—tenofovir, bepotastine, epirubicin, epoprostenol, tirazavirin, aprepitant and valrubicin are studied by using DFT methodology. The geometry optimization of these potential inhibitors is performed with the help of computational software Gaussian 16 within density functional theory framework [50]. For optimization, hybrid functional Becke-three parameter Lee-Yang-Parr (B3LYP) with basis set 6-311G (d,p) is selected. However, it is established that conventional DFT underestimates the HOMO/LUMO energy levels and application of non-empirical range-separated functional can recover the correct energy levels. Non-empirical range-separated functional give better accuracy as compared to the conventional functional for biomolecules [51,52].

Currently, for calculation of solvation energies and binding free energies of small to medium molecules a number of quantum chemical techniques are being used. However, these methods are not appropriate for large molecular system of protein or protein-protein interactions or target-based drug findings [53]. It is reported that polarizable continuum model (PCM) and isodensity-polarizable-continuum model (I-PCM) provide much better results by using DFT technique with hybrid exchange correlation—B3LYP or the MP2 technique using TDFT. However, I-PCM is a time consuming, expensive and highly intensive computational technique and may not be compatible with PPIs and protein-drug molecular system. Alternatively, the Onsager computational model is cost effective and requires less computational effort, provided that the vital position is obtained with the help of molecular docking technique or classical molecular dynamics. The Onsager model does not provide result as accurately as IPCM or PCM models, but it offers an economical substitute when IPCM or PCM are not possible for PPIs or large protein molecular system [24]. It works well with basis sets such as 6-311G(d,p), aug-cc-pVTZ *etc*. In this case, Onsager model may provide suitable results with functional B3LYP and basis set 6-311G (d,p) for potential inhibitors—tenofovir, bepotastine, epirubicin, epoprostenol, tirazavirin, aprepitant and valrubicin.

Ionization Potential (I) and Electron Affinity (A) of these compounds are calculated with the help of Koopman's theorem by using following equations [54]:

$$I = -\varepsilon_{\text{HOMO}}, \tag{1}$$

$$A = -\varepsilon_{\text{LUMO}}, \tag{2}$$

The conceptual DFT based global descriptors viz., molecular hardness (η), softness (S), electronegativity (χ), electrophilicity index (ω) and nucleophilicity index are computed as below:

$$\chi = -\mu = \frac{I + A}{2}, \tag{3}$$

where, μ represents the chemical potential of the system.

$$\eta = \frac{I - A}{2}, \tag{4}$$

$$S = \frac{1}{2\eta}, \tag{5}$$

$$\omega = \frac{\mu^2}{2\eta}, \tag{6}$$

$$N = \frac{1}{\omega}. \tag{7}$$

ACKNOWLEDGEMENTS

We would like to thank Manipal University Jaipur and Sharda University for providing computational facilities and research support.

COMPLIANCE WITH ETHICS GUIDELINES

The authors Prabhat Ranjan, Kumar Gaurav and Tanmoy Chakraborty declare that they have no conflict of interest or financial conflicts to disclose. All procedures performed in studies involving animals were in accordance with the ethical standards of the institution or practice at which the studies were conducted, and with the 1964 Helsinki declaration and its later amendments or comparable ethical standards.

REFERENCES

1. Kumar, A., Kumar, D., Kumar, R., Singh, P., Chandra, R. and Kumari, K. (2020) DFT and docking studies of designed conjugates of noscapines & repurposing drugs: promising inhibitors of main protease of SARS-CoV-2 and falcipan-2. J. Biomol. Struct. Dyn., doi: 10.1080/07391102.2020.1841030
2. Ahmed, K., Aldosouky, M., Ali, S. M., Aftab, Z. and Zarour, A. (2020) Acute care surgery fellowship program acclimatization to

the COVID-19 pandemic: Experience from Qatar. Br. J. Surg., 107, e666
3. Al-Mandhari, A. (2020) Coming together in the region to tackle COVID-19. East. Mediterr. Health J., 26, 992−993
4. Al-Tawfiq, J. A., Sattar, A., Al-Khadra, H., Al-Qahtani, S., Al-Mulhim, M., Al-Omoush, O. and Kheir, H. O. (2020) Incidence of COVID-19 among returning travelers in quarantine facilities: A longitudinal study and lessons learned. Travel Med. Infect. Dis., 38, 101901
5. Atal, S., Fatima, Z. and Balakrishnan, S. (2020) Approval of itolizumab for COVID-19: A premature decision or need of the hour? BioDrugs, 34, 705–711
6. Bakouny, Z., Hawley, J. E., Choueiri, T. K., Peters, S., Rini, B. I., Warner, J. L. and Painter, C. A. (2020) COVID-19 and cancer: Current challenges and perspectives. Cancer Cell, 38, 629−646
7. Berekaa, M. M. (2021) Insights into the COVID-19 pandemic: Origin, pathogenesis, diagnosis, and therapeutic interventions. Front. Biosci. (Elite Ed.), 13, 117−139
8. Dublin, S., Walker, R. L., Floyd, J. S., Shortreed, S. M., Fuller, S., Albertson-Junkans, L., Harrington, L. B., Greenwood-Hickman, M. A., Green, B. B. and Psaty, B. M. (2021) Renin-angiotensin-aldosterone system inhibitors and COVID-19 infection or hospitalization: A cohort study. Am. J. Hypertens., 34, 339−347
9. Sanders, J. M., Monogue, M. L., Jodlowski, T. Z. and Cutrell, J. B. (2020) Pharmacologic treatments for coronavirus disease 2019 (COVID-19). JAMA, 323, 1824−1836
10. Zhu, N., Zhang, D., Wang, W., Li, X., Yang, B., Song, J., Zhao, X., Huang, B., Shi, W., Lu, R., *et al*. (2020) A novel coronavirus from patients with pneumonia in China, 2019. N. Engl. J. Med., 382, 727−733
11. Hooshmand, S. A., Ghobadi, M. Z., Hooshmand, S. E., Jamalkandi, S. A., Alavi, S. M. and Masoudi-Nejad, A. (2020) A multimodal deep learning-based drug repurposing approach for treatment of COVID-19. Mol. Divers., 25, 1717−1730
12. Hsieh, K., Wang, Y., Chen, L., Zhao, Z., Savitz, S., Jiang, X., Tang, J. and Kim, Y. (2020) Drug repurposing for COVID-19 using graph neural network with genetic, mechanistic, and epidemiological validation. Res. Sq., doi: 10.21203/rs.3.rs-114758/v1
13. Ino, H., Nakazawa, E. and Akabayashi, A. (2021) Drug repurposing for COVID-19: Ethical considerations and roadmaps. Camb. Q. Healthc. Ethics, 30, 51−58
14. Koren, G. and Korn, L. (2020) Chloroquine for Covid 19: introducing drug repurposing to medical students. Int. J. Med. Educ., 11, 155−157
15. Mahdian, S., Ebrahim-Habibi, A. and Zarrabi, M. (2020) Drug repurposing using computational methods to identify therapeutic options for COVID-19. J. Diabetes Metab. Disord., 19, 691−699
16. Masoudi-Sobhanzadeh, Y. (2020) Computational-based drug repurposing methods in COVID-19. Bioimpacts, 10, 205−206
17. Meyer-Almes, F. J. (2020) Repurposing approved drugs as potential inhibitors of 3CL-protease of SARS-CoV-2: Virtual screening and structure based drug design. Comput. Biol. Chem., 88, 107351
18. Mucke, H. A. M. (2020) COVID-19 and the drug repurposing tsunami. Assay Drug Dev. Technol., 18, 211−214
19. Soufi, G. J. and Iravani, S. (2021) Potential inhibitors of SARS-CoV-2: Recent advances. J. Drug Target., 29, 349−364
20. Soufi, G. J., Hekmatnia, A., Nasrollahzadeh, M., Shafiei, N., Sajjadi, M., Iravani, P., Fallah, S., Iravani, S. and Varma, R. S. (2020) SARS-CoV-2 (COVID-19): New discoveries and current challenges. Appl. Sci. (Basel), 10, 3641
21. Nasrollahzadeh, M., Sajjadi, M., Soufi, G. J., Iravani, S. and Varma, R. S. (2020) Nanomaterials and nanotechnology-associated innovations against viral infections with a focus on coronaviruses. Nanomaterials (Basel), 10, 1072
22. Tu, Y. F., Chien, C. S., Yarmishyn, A. A., Lin, Y. Y., Luo, Y. H., Lin, Y. T., Lai, W. Y., Yang, D. M., Chou, S. J., Yang, Y. P., *et al*. (2020) A review of SARS-CoV-2 and the ongoing clinical trials. Int. J. Mol. Sci., 21, 2657
23. Ramkumar, G. R., Srinivasan, S., Bhoopathy, T. J. and Gunasekaran, S. (2012) Vibrational spectroscopic studies of tenofovir using density functional theory method. J. Chem., 2013, 126502
24. Patil, V. M., Narkhede, R. R., Masand, N., Cheke, R. S. and Balasubramanian, K. (2020) Molecular insights into resveratrol and its analogs as SARS-CoV-2 (COVID-19) protease inhibitors. Coronaviruses, 2, 10−27
25. Jarange, A. B., Patil, S. V., Malkhede, D. D., Deodhar, S. M., Nandre, V. S., Athare, S. V., Kodam, K. M. and Gejji, S. P. (2021) *p*-sulfonatocalixarene versus *p*-thiasulfonatocalixarene: encapsulation of tenofovir disoproxil fumarate and implications to ESI-MS, HPLC, NMR, DFT and anti-MRSA activities. J. Incl. Phenom. Macrocycl. Chem., 99, 43−59
26. Elfiky, A. A. (2020) Ribavirin, remdesivir, sofosbuvir, galidesivir, and tenofovir against SARS-CoV-2 RNA dependent RNA polymerase (RdRp): A molecular docking study. Life Sci., 253, 117592
27. Toroz, D. and Gould, I. R. (2019) A computational study of anthracyclines interacting with lipid bilayers: Correlation of membrane insertion rates, orientation effects and localisation with cytotoxicity. Sci. Rep., 9, 2155
28. Sobczak, A., Lesniewska-Kowiel, M. A., Muszalska, I., Firlej, A., Cielecka-Piontek, J., Tomczak, S., Barszcz, B., Oszczapowics, I. and Jelinkska, A. (2017) Stability of epidoxorubicin hydrochloride in aqueous solutions: Experimental and theoretical studies. J. Chem., 2017, 8107140
29. Samide, A., Tutunaru, B., Varut, R. M., Oprea, B. and Iordache, S. (2021) Interactions of some chemotherapeutic agents as epirubicin, gemcitabine and paclitaxel in multicomponent systems based on orange essential oil. Pharmaceuticals (Basel), 14, 619
30. Liu, X. and Wang, X. J. (2020) Potential inhibitors against 2019-nCoV coronavirus M protease from clinically approved medicines. J. Genet. Genomics, 47, 119−121
31. Wang, J. (2020) Fast identification of possible drug treatment of coronavirus disease-19 (COVID-19) through computational drug

repurposing study. J. Chem. Inf. Model., 60, 3277−3286
32. O'Boyle, N. M., Tenderholt, A. L. and Langner, K. M. (2008) cclib: a library for package-independent computational chemistry algorithms. J. Comput. Chem., 29, 839−845
33. Ghosh, D. C. and Bhattacharyya, S. (2004) Molecular orbital and density functional study of the formation, charge transfer, bonding and the conformational isomerism of the boron trifluoride (BF3) and ammonia (NH3) donor-acceptor complex. Int. J. Mol. Sci., 239, 5
34. Parr, R. G. and Chattaraj, P. K. (1991) Principle of maximum hardness. J. Am. Chem. Soc., 113, 1854−1855
35. Chattaraj, P. K. and Sengupta, S. (1999) Chemical hardness as a possible diagnostic of the chaotic dynamics of rydberg atoms in an external field. J. Phys. Chem., 103, 6122−6126
36. Sanderson, R. T. (1951) An interpretation of bond lengths and a classification of bonds. Science, 114, 670−672
37. Sanderson, R. T. (1952) Carbon–carbon bond lengths. Science, 116, 41−42
38. Sanderson, R. T. (1955) Partial charges on atoms in organic compounds. Science, 121, 207−208
39. Sanderson, R. T. (1952) Electronegativities in inorganic chemistry. J. Chem. Educ., 29, 539
40. Sanderson, R. T. (1954) Electronegativities in inorganic chemistry. III. J. Chem. Educ., 31, 238
41. Sanderson, R. T. (1960) Chemical Periodicity. New York: Reinhold Publishing Corporation
42. Vleeschouwer, F. D., Speybroeck, V. V., Waroquier, M., Geerlings, P. and Proft, F. D. (2007) Electrophilicity and nucleophilicity index for radicals. Org. Lett., 9, 2721
43. Elfiky, A. A. (2020) SARS-CoV-2 RNA dependent RNA polymerase (RdRp) targeting: An *in silico* perspective. J. Biomol. Struct. Dyn., 2020, 1−9
44. Hasan, M. K., Kamruzzaman, M., Bin Manjur, O. H., Mahmud, A., Hussain, N., Alam Mondal, M. S., Hosen, M. I., Bello, M. and Rahman, A. (2021) Structural analogues of existing anti-viral drugs inhibit SARS-CoV-2 RNA dependent RNA polymerase: A computational hierarchical investigation. Heliyon, 7, e06435
45. Salpini, R., Alkhatib, M., Costa, G., Piermatteo, L., Ambrosio, F. A., Di Maio, V. C., Scutari, R., Duca, L., Berno, G., Fabeni, L., *et al*. (2021) Key genetic elements, single and in clusters, underlying geographically dependent SARS-CoV-2 genetic adaptation and their impact on binding affinity for drugs and immune control. J. Antimicrob. Chemother., 76, 396−412
46. Yun, Y., Song, H., Ji, Y., Huo, D., Han, F., Li, F. and Jiang, N. (2020) Identification of therapeutic drugs against COVID-19 through computational investigation on drug repurposing and structural modification. J. Biomed. Res., 34, 458−469
47. Toor, H. G., Banerjee, D. I., Lipsa Rath, S. and Darji, S. A. (2021) Computational drug re-purposing targeting the spike glycoprotein of SARS-CoV-2 as an effective strategy to neutralize COVID-19. Eur. J. Pharmacol., 890, 173720
48. Cole, D. J. and Hine, N. D. M. (2016) Applications of large-scale density functional theory in biology. J. Phys. Condens. Matter, 28, 393001
49. Sulpizi, M., Folkers, G., Rothlisberger, U., Carloni, P. and Scapozza, L. (2002). Mol. Inform., 21, 173
50. Gaussian 16, Revision A.03. (2016) Gaussian, Inc., Wallingford CT
51. Foster, M. E. and Wong, B. M. (2012) Nonempirically tuned range-separated DFT accurately predicts both fundamental and excitation gaps in DNA and RNA nucleobases. J. Chem. Theory Comput., 8, 2682−2687
52. Sun, H., Zhang, S., Zhong, C. and Sun, Z. (2016) Theoretical study of excited states of DNA base dimers and tetramers using optimally tuned range-separated density functional theory. J. Comput. Chem., 37, 684−693
53. Balasubramanian, K. (2021) Computational and artificial intelligence techniques for drug discovery and administration. Biomed. Sci., doi:10.1016/B978-0-12-820472-6.00015-3
54. Parr, R. G. and Yang, W. (1989) Density Functional Theory of Atoms and Molecules. New York: Oxford University Press